KNEE

Small differences in tibial contact locations following kinematically aligned TKA from the native contralateral knee

Stephanie Nicolet-Petersen[1] · Augustine Saiz[2] · Trevor Shelton[2] · Stephen M. Howell[1] · Maury L. Hull[1,2,3]

Abstract

Purpose Kinematically aligned (KA) TKA strives to restore native limb and knee alignments without ligament release with the premise that knee function likewise will be closely restored to native to the extent enabled by the components used. This study determined differences in anterior–posterior (AP) tibial contact locations of a KA TKA performed with asymmetric, fixed bearing, posterior cruciate-retaining (PCR) components from those of the native contralateral knee and also determined the incidence of posterior rim contact of the tibial insert during a deep knee bend and a step-up.

Methods Both knees were imaged using single-plane fluoroscopy for 25 patients with a calipered KA TKA and a native knee in the contralateral limb. AP tibial contact locations in each compartment were determined following 3D model-to-2D image registration. Differences in mean AP tibial contact locations in each compartment between the KA TKA knees and the native contralateral knees were analysed. Contact locations either on or beyond the most posterior point of the tibial insert determined the occurrence of posterior rim contact.

Results Mean AP tibial contact locations for both native and KA TKA knees remained relatively centred in the medial compartment but moved posterior in the lateral compartment during flexion. In both the medial and lateral compartments, differences in mean AP tibial contact locations between the KA TKA knees and the native contralateral knees were more posterior and greatest at 0° flexion for both activities (4 mm, $p = 0.0009$ and 7 mm, $p < 0.0001$ for deep knee bend and 6 mm, $p < 0.0001$ and 8 mm, $p < 0.0001$ for step-up in the medial and lateral compartments, respectively). The incidence of posterior rim contact of the tibial insert was 16% (4 of 25 patients) but the lowest Oxford Knee Score was 43 for these patients. The median Oxford Knee Score for all patients was 46 (out of 48).

Conclusions Calipered KA TKA with asymmetric, fixed bearing, PCR components resulted in mean AP tibial contact locations which were relatively centred in the compartments and differed at most from those of the native contralateral knee by approximately 15% of the AP dimension of a mid-sized tibial baseplate. Although posterior rim contact occurred in some patients, all such patients had high patient-reported outcome scores.

Level of evidence Therapeutic, Level III.

✉ Maury L. Hull
mlhull@ucdavis.edu

1 Department of Biomedical Engineering, University of California Davis, One Shields Avenue, Davis, CA 95616, USA

2 Department of Orthopaedic Surgery, University of California Davis Medical Center, 4860 Y Street, Suite 3800, Sacramento, CA 95817, USA

3 Department of Mechanical Engineering, University of California Davis, One Shields Avenue, Davis, CA 95616, USA

Introduction

The surgical goal of kinematically aligned (KA) total knee arthroplasty (TKA) is to align the joint lines of the components with those of the native (i.e. pre-arthritic) knee which avoids ligament release [13]. In contrast to mechanically aligned (MA) TKA, which strives for neutral coronal limb alignment for all patients, KA TKA strives to restore the limb and knee alignment to that of the native knee for each patient individually. The latest support for kinematic or an 'individualized' alignment approach in place of mechanical

alignment is based on the new systematic classification of the phenotypes of the native limb and knee joint line [11]. 3D-reconstructed CT images confirmed the great variability of the coronal alignment of the lower limb and joint lines in both non-osteoarthritic [22] and osteoarthritic knees [10]. The currently used classification system (neutral, varus, valgus) oversimplifies the coronal alignment, and should be replaced by the use of femoral and tibial phenotypes. The detailed phenotype assessment of a patient's individual anatomy justifies the individualised approach to TKA of restoring the native joint lines and limb alignment, which is the goal of KA TKA.

The premise behind the kinematic alignment approach is that knee function will be closely restored to that of the native (i.e. pre-arthritic) knee to the extent enabled by the particular component design used. Using asymmetric, fixed bearing, posterior cruciate-retaining (PCR) components, KA TKA results in biomechanical variables characterising tibiofemoral joint function in passive motion such as laxities [32] and tibial contact forces [31] which are not different generally from those of the native knee. However, biomechanical variables characterising tibiofemoral joint function during dynamic weight-bearing activities of daily living following KA TKA have not been determined so that the extent to which KA TKA restores tibiofemoral joint function to that of the native knee in activities of daily living remains unknown using these components.

Based on 3D model-to-2D image registration of fluoroscopic images, the anterior–posterior (AP) tibial contact locations in the medial and lateral compartments during activities of daily living can be determined and serve as objective biomechanical variables characterising knee function following TKA. Although tibial contact locations after KA TKA performed with asymmetric, fixed bearing, PCR components should not be identical to those of the native knee because of differences in curvature of the articular surfaces and the absence of the ACL, nevertheless differences in AP tibial contact locations between a KA TKA with these components and a native knee should be limited as should the incidence of posterior rim contact of the tibial insert. Posterior rim contact occurs when either the lateral or the medial femoral condyle contacts the rim surrounding the concavity forming the articular surface of a compartment in the tibial insert. Posterior rim contact has been associated with complications such as accelerated, uneven wear of the insert [9].

A previous static analysis of AP tibial contact locations in KA TKA using symmetric, fixed bearing, PCR components during kneeling showed no incidence of posterior rim contact of the tibial insert [12]. However, the differences in AP tibial contact locations between a KA TKA performed with asymmetric, fixed bearing, PCR components and the native contralateral knee and the incidence of posterior rim contact of the tibial insert are unknown during dynamic activities of daily living.

Accordingly, this study determined differences in AP tibial contact locations between those of a KA TKA performed with asymmetric, fixed bearing, PCR components and those of the native contralateral knee and also determined the incidence of posterior rim contact of the tibial insert during a deep knee bend and a step-up. This study also reported the overall patient function at a minimum follow-up of 14 months as measured by the Oxford Knee, Knee Society, Forgotten Joint, WOMAC, and UCLA Scores. Our primary hypothesis was that the mean AP tibial contact locations for KA TKA using the component design above would not differ markedly from those for the native knee. If this hypothesis was accepted, then this result would confirm the premise of KA TKA and help explain the relatively high patient-reported outcome scores previously reported for KA TKA [4, 6, 18].

Methods

Patients

This study was approved by the Institutional Review Board at the University of California, Davis (IRB# 954288). Inclusion criteria were patients having KA TKA performed with asymmetric, fixed bearing, PCR components (Persona CR, Zimmer-Biomet, Warsaw, IN), a native contralateral limb with no evidence of degenerative joint disease, no skeletal abnormalities or prior surgery in either limb except for the KA TKA, no history of rheumatic or traumatic arthritis, age between 40 and 85 years, a Body Mass Index less than or equal to 40, ability to perform activities of daily living without discomfort in the native contralateral limb, and ability to have an MR scan of the native contralateral limb. Note that patients were selected with no restriction on pre-operative varus–valgus or flexion contracture deformity.

Patients considered for inclusion were those operated on between November 2014 and April 2017 by one surgeon who performed calipered KA TKA on 1201 consecutive patients. Patients were winnowed down to those meeting the inclusion criteria in a three-step process. The first step entailed a review of medical records to identify those patients within the age range and BMI range and those with acceptable medical history. The second and third steps involved a review of CT images. Post-operative AP and lateral CT scanograms of both limbs and CT axial images of both knees were obtained with the Perth protocol. The second step involved a review of the scanograms to identify those patients with a unilateral calipered KA TKA without a skeletal abnormality in either limb. The third step involved a review of multiplane reconstructions of the axial images to

Table 1 Pre-operative demographic patient data for those patients imaged ($N=25$) and those not imaged ($N=66$)

Parameters	Imaged ($N=25$)	Not imaged ($N=66$)	Significance
Pre-operative clinical characteristics			
Age (years)	64 ± 7 (52–82)	66 ± 7 (50–81)	$p=0.258$
Sex (male) N (%)	14 (56%)	34 (52%)	$p=0.815$
Body Mass Index (kg/m^2)	29 ± 5 (22–40)	29 ± 5 (18–39)	$p=0.993$
Pre-operative knee conditions			
Knee extension (°)	10 ± 8 (0–27)	14 ± 7 (0–30)	$p=0.021$
Knee flexion (°)	115 ± 7 (95–125)	114 ± 8 (90–130)	$p=0.506$
Valgus (−)/varus (+) deformity (°)	0.1 ± 8 (− 15 to 13)	-0.2 ± 10 (− 22 to 25)	$p=0.762$
Pre-operative function			
Oxford Knee Score (48 best, 0 worst)	23 ± 8 (4–38) median: 24	20 ± 7 (5–36) median: 21	$p=0.052$
Knee Society Score (100 best, 0 worst)	34 ± 10 (14–59) median: 32	31 ± 16 (8–94) median: 29	$p=0.116$

Note that the number not imaged is one less than the actual number not imaged ($N=67$) because the complete data in the table were not available for one patient not imaged. Data are given as mean ± standard deviation (range) unless noted otherwise

Wilcoxon rank-sum test used to determine p values for differences in means. Fisher's exact test used to determine p values for differences in proportions. Significance set at $p<0.05$

identify those patients without subchondral sclerosis, joint space narrowing, marginal osteophytes, and subchondral cysts of the tibiofemoral and patellofemoral joints in the unoperated knee. From these three steps, 92 patients were identified who met the inclusion criteria.

Patients meeting the inclusion criteria were contacted at random until 31 agreed to participate and gave informed consent. Of those who gave informed consent, 2 were excluded due to the presence of osteoarthritis on MRI or standing AP fluoroscopic image, 1 was excluded due to lost data on the fluoroscope, 2 were excluded due to having a different implant design and the pilot patient was excluded due to technical problems, which left 14 males and 11 females who participated in the study (Table 1). The level of pre-operative osteoarthritis and kinematic dysfunction of the knees of the final 25 patients tested was severe as evidenced by 68% ($N=17$) and 28% ($N=7$) having either a grade 4 or 3 Kellgren–Lawrence radiologic classification of osteoarthritis on a standing full extension or 30°–45° knee flexion view, and 28% ($N=7$) and 8% ($N=2$) having either a torn ACL or a non-functional ACL reconstruction at the time of surgical exposure.

Surgical technique

Using ten sequential caliper measurements and a series of verification checks with manual instruments, KA TKA was performed by a single surgeon using a mid-vastus approach following a previously described technique [24]. Asymmetric, fixed bearing, PCR-retaining components and a patella button were implanted with cement (Persona CR, Zimmer Biomet, Warsaw, IN). For the femoral component, the varus–valgus orientation and proximal–distal location were set to restore the native distal femoral joint line by adjusting the thickness of the distal femoral resections as measured with a caliper to within 0 ± 0.5 mm of the thickness of the femoral component condyles after compensating for cartilage wear and saw blade kerf. The internal–external orientation and anterior–posterior location were set to restore the native posterior joint line by adjusting the thickness of the posterior femoral resections as for the distal femoral joint line. These steps set the femoral component with a bias of 0.3° and precision of $\pm1.1°$ with respect to the flexion–extension plane of the knee [23].

For the tibial component, the varus–valgus orientation was set to restore the native joint line by insuring that the thicknesses measured with a caliper at the base of the tibial spines medially and laterally was within 0 ± 0.5 mm. With the knee in full extension, the varus–valgus angle of the tibial resection was fine tuned until the varus–valgus laxity was negligible as in the native knee [30]. The internal–external rotation of the tibial component was set using a kinematic tibial template with a negligible bias of 0.1° external and a precision of $\pm3.9°$ [26]. With the knee in 90° of flexion, the slope was set to restore the native joint line in the medial compartment so that the offset of the anterior tibia from the distal medial femoral condyle with trial components matched that of the knee at exposure after adjusting for cartilage wear on the femur and insuring that the internal–external laxity approximated 14° as in the native knee [30]. Ligament releases were not performed. This surgical procedure restores the hip–knee–ankle angle, distal lateral femoral angle, and proximal medial tibial angle to native within $\pm3°$ with frequencies of 95%, 97% and 97%, respectively [24].

With trial components and the knee in 90° of flexion, the competency of the posterior cruciate ligament (PCL) was confirmed. This confirmation consisted of a visual inspection determining no detachment of the insertion or saw blade laceration, a manual palpation detecting tension, and a measurement of the AP offset matching that of the knee at the time of surgical exposure.

Data collection

Fluoroscopic images (OEC 9900 Elite, General Electric, Boston, MA) were recorded for each patient's native and KA TKA knees in an oblique sagittal orientation of approximately 10°–15° at 15 frames per second whilst they performed a deep knee bend from full extension to maximum flexion, and again whilst they performed a step-up. First, all noise reduction functions on the fluoroscope were disabled. Next, the patient's knee under study was statically imaged with the automatic brightness and contrast setting enabled on the fluoroscope to adjust the imaging parameters specific to the patient's anatomy. When the image was deemed suitable in terms of brightness and contrast, these parameters were fixed and the dynamic images were collected. The oblique sagittal orientation was used to better register the 3D model to the 2D images by making the silhouette produced exhibit distinguishing features of the 3D model in the sagittal and coronal planes [29]. For the deep knee bend, patients staggered their stance in the AP direction to prevent the contralateral knee from impeding the view of the knee under study, and to keep both feet planted on the platform. For the step-up, patients placed the foot of the limb under study on a 22 cm high step and lifted themselves as though they were climbing a set of stairs, but did not follow through with the contralateral limb, again to prevent obstructing the view of the knee under study. Patients performed the activities over 5–7 s to reduce motion blur. Hand rails were provided to aid in stability.

With the patient lying supine, the native knee was imaged with a 3T MRI (TIM Trio, Siemens, Munich, Germany) with dedicated knee surface coil and 1 mm thick sagittal plane slices (flip angle $= 12°$, 256×256 pixel resolution interpolated to 512×512, $0.8 \times 0.8 \times 1.0$ mm voxel size, $TR = 17$ ms, $TE = 4$ ms). The MRI images were imported into commercially available software (Mimics v20.0, Materialise, Belgium) and segmented to create three-dimensional (3D) models of the distal femur and proximal tibia/fibula. After the MR scan with the patient still lying supine, the passive limits of extension and flexion were measured in each knee. Patient-reported outcome scores were obtained at the time of imaging.

Data processing

Fluoroscopic images were corrected for distortion after which images at 0°, 30°, 60°, 90° and maximum flexion were identified for the deep knee bend and images at 0°, 15°, 30°, 45° and 60° were identified for the step-up. Images were subsequently filtered for noise using a pixel-wise adaptive low-pass Wiener filter in Matlab (Mathworks, Natick, MA). The in vivo 3D position and orientation of the patient-specific bone models developed from the MR images and the manufacturer-supplied component models were determined using 3D model-to-2D image registration techniques [1] and open-source software (https://sourceforge.net/projects/jointtrack/). The bone and component models were projected onto the fluoroscopic images and iteratively adjusted in six degrees of freedom until their silhouettes most closely matched their silhouettes in the image. For the component models, the high contrast of the metallic components provided detailed edge information, and an automated optimization routine determined the final orientation and in-plane position [1, 17]. For the bone models, the optimum registration was determined manually because inconsistent edge definition in the native knee images frequently resulted in visible errors in rotations and in-plane translations when the optimization routine was executed. The bone models included internal features, specifically the occluded condyles of the femur, tibial plateau and fibular head to improve registration accuracy [21]. The femur/femoral component was then translated in the out-of-plane direction until it was centred on top of the tibia/tibial component (Fig. 1). This step was necessary given that the out-of-plane translation errors encountered in single-plane fluoroscopy can result in the reconstruction of physiologically impossible poses [7, 27].

Coordinate systems were established on the tibial plateau for the native knee and the tibial baseplate for the TKA knee to report the AP tibial contact locations. The 3D models of the native femur and tibia were imported into commercial software (Geomagic Control, 3D Systems, Cary, NC) in the same position and orientation that they were in the patient during the MR scan. The posterior surfaces of the femoral condyles were superimposed to define the sagittal plane and the same transformation was applied to the tibia. The axial plane was parallel to the medial tibial articular surface and perpendicular to the sagittal plane. The centre of a bounding box drawn around the tibial plateau in the axial view defined the origin of the tibial coordinate system in the native knee. Similarly, the axial plane of the tibial baseplate was parallel to the transverse plane of the baseplate, and the centre of a bounding box drawn around the baseplate in the axial view defined the origin of the tibial coordinate system in the KA TKA knee (Fig. 2).

The AP tibial contact locations in the medial and lateral compartments for the KA TKAs were computed as the
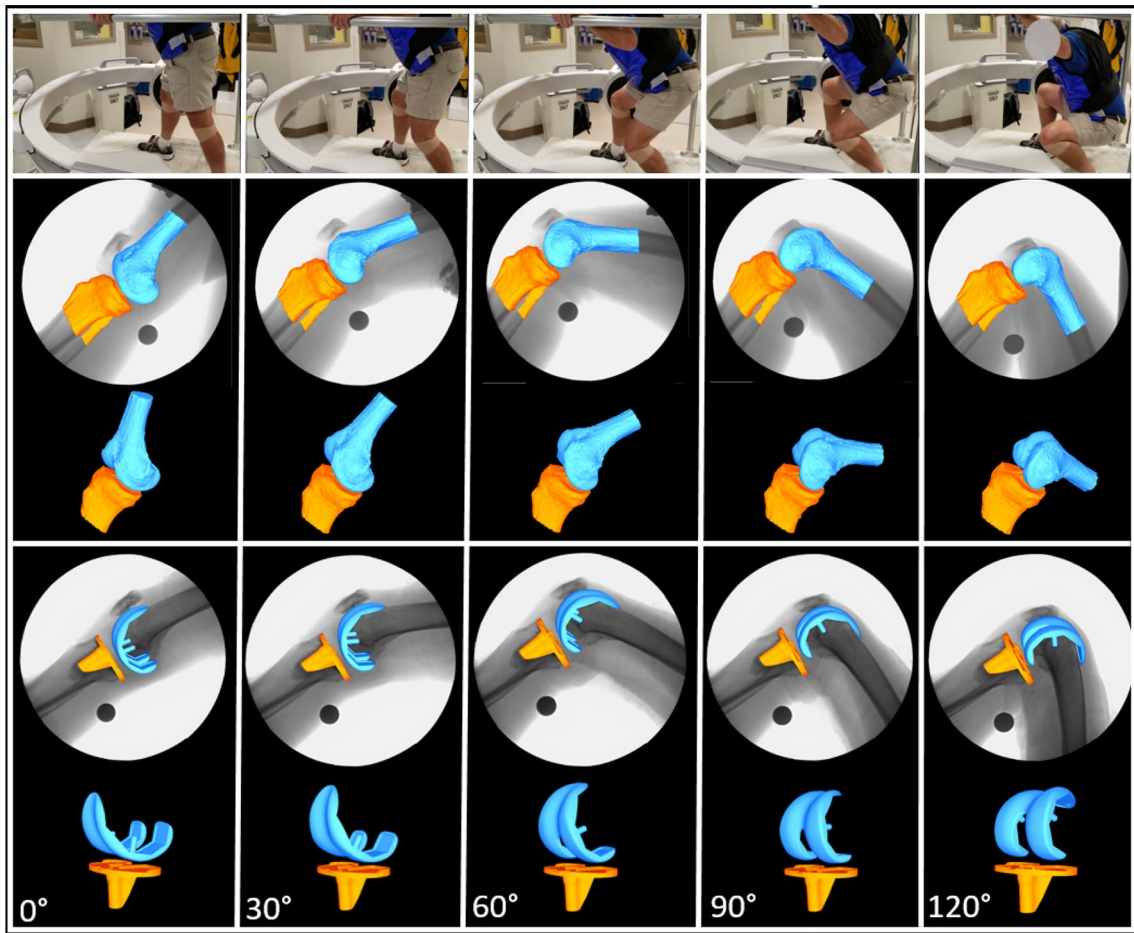
Fig. 1 Composite shows images of a patient performing a deep knee bend from full extension to maximum flexion (top row), 3D model-to-2D image registration and the 3D position and orientation of the femur and tibia after registration and out-of-plane centering for the native knee (middle row), and 3D model-to-2D image registration and the 3D position and orientation of the femoral and tibial components after registration and out-of-plane centering for a KA TKA (bottom row)
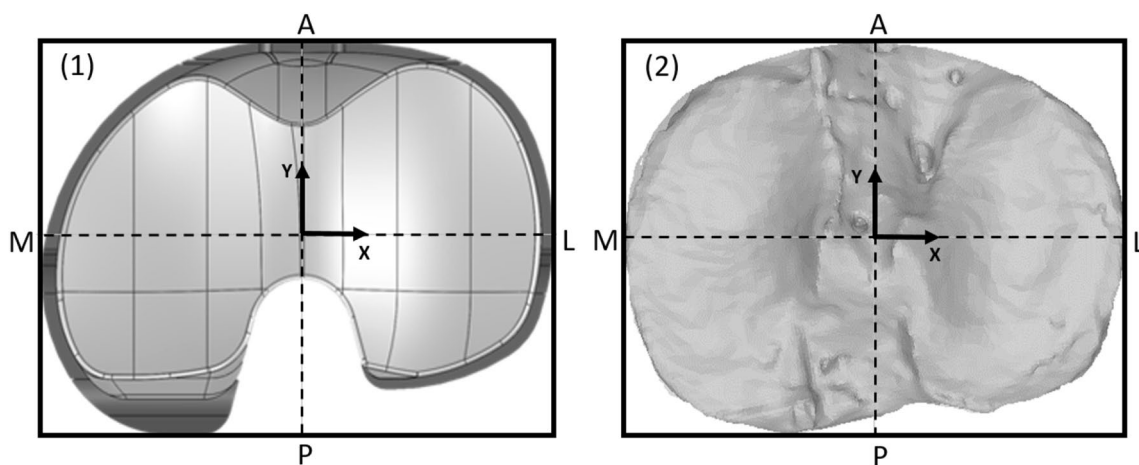

Fig. 2 Axial views of a right proximal tibial component (1) and right proximal tibial plateau (2) show the tibial coordinate systems used to report AP tibial contact locations in the medial and lateral compartments. The centres of the bounding boxes around the component and plateau in the axial view define the origins of the coordinate systems. The x-axes are the medial–lateral axes and the y-axes are the AP axes of the tibial component and native tibia. Note that aligning the asymmetric tibial component kinematically by superimposing the x- and y-axes leaves the lateral tibial plateau uncovered posteriorly

lowest points on the femoral condyles relative to the transverse plane of the tibial baseplate. Because this method references only the transverse plane of the baseplate and does not take into account the AP dimensions of the baseplate or insert, it is possible that the lowest point on a femoral condyle could lie outside of the AP dimensions of the insert even if the condyle actually contacts the rim of the insert. Accordingly, a lowest point within 1 mm of or beyond the most posterior point of the medial or lateral compartment of the insert after correcting for the bias error inherent to the lowest point method [29] determined the occurrence of posterior rim contact of the tibial insert. The AP tibial contact location in a compartment for the native knee was computed as the geometric centroid of all points on the subchondral bone of a femoral condyle having a separation of 6 mm or less from the subchondral bone beneath the tibial articular surface [20, 35]. All AP tibial contact locations were standardised to the 53 mm AP dimension of the mid-sized tibial baseplate (Size F, Persona CR, Zimmer-Biomet) by multiplying each patient's AP tibial contact locations by the ratio of the AP dimension of the mid-sized baseplate to the AP dimension of their implanted baseplate or native tibial plateau.

Statistical analysis

The arithmetic mean and standard deviation were used to describe the AP tibial contact locations in the medial and lateral compartments at each flexion angle for both knee conditions and the demographic data across all 25 patients (Table 1). The median and range were used to describe the patient-reported outcome measures (Oxford Knee, Knee Society, Forgotten Joint, WOMAC and UCLA Scores). Paired t tests determined the differences in mean AP tibial contact locations between the KA TKAs and the native contralateral knees in each of the medial and lateral compartments at each flexion angle.

A power analysis confirmed that with 25 patients, a difference in the AP tibial contact locations in the medial and lateral compartments between the KA TKA knees and the native knees of 4 mm, which is less than 10% of the AP dimension of the mid-sized tibial baseplate to which all data were standardised, could be detected with $\alpha = 0.05$ and $(1 - \beta) \geq 0.80$ using a standard deviation of the differences in AP tibial contact locations in the lateral compartment of 6.8 mm. This value was obtained from the present study based on measurements from 10 patients and subsequently checked with measurements from all 25 patients.

An intraclass correlation coefficient (ICC) analysis was performed to determine the repeatability and reproducibility of the manual native knee registration method. Five patients were randomly selected and 3D model-to-2D image registration was performed on their native knee images at 30° and

Table 2 Patient-reported outcome scores at the time of imaging ($N = 25$)

Patient-reported outcome scores	Median (range)
Oxford Knee Score (48 best, 0 worst)	46 (28–48)
WOMAC Score (0 best, 96 worst)	3 (0–43)
Forgotten Joint Score (100 best, 0 worst)	75 (2–100)
Knee Society Score (150 best, −20 worst)	140 (80–150)
UCLA Score (10 best, 1 worst)	7 (5–10)

90° of flexion. Three observers performed the registration five times with at least 24 h between trials. The AP tibial contact locations were computed for each trial and each observer, and a two-factor analysis of variance (ANOVA) was performed at each flexion angle where the two factors were observer at three levels and patient at five levels. Observer and patient were modelled as random effects (JMP, SAS Institute Inc., Cary, NC). The resulting variance components for observer, subject (patient), and error were used to compute the intraobserver and interobserver ICCs [3]. An ICC value of > 0.9 indicates excellent agreement, 0.75–0.90 indicates good agreement, 0.5–0.75 indicates moderate agreement and 0.25–0.5 indicates fair agreement [15].

Results

Patient-reported outcome scores

The median patient-reported outcome scores were 46 for the Oxford Knee Score, 3 for the WOMAC, 75 for the Forgotten Joint Score, 140 for the Knee Society Score and 7 for the UCLA Score (Table 2).

Deep knee bend

In the medial and lateral compartments at 0° of flexion, the mean AP tibial contact locations of the KA TKA knees were 4 mm and 7 mm more posterior than those of the native knees, respectively ($p = 0.0009$, $p < 0.0001$). At 30°, 60°, 90° and maximum flexion, the difference in the mean AP tibial contact locations was 3 mm or less even when significant (medial compartment 90° and max: $p = 0.0021$, $p = 0.0062$; lateral compartment 30° and 60°: $p = 0.0026$, $p = 0.0107$). Qualitatively, the mean contact locations in the medial and lateral tibial compartments fell in the same regions between the KA TKA knees and the native knees at all flexion angles greater than 0° (Fig. 3).

The incidence of posterior rim contact of the tibial insert in the lateral compartment was 12% (3 of 25 patients). Posterior rim contact developed as Patients 3 and 21 reached 60°
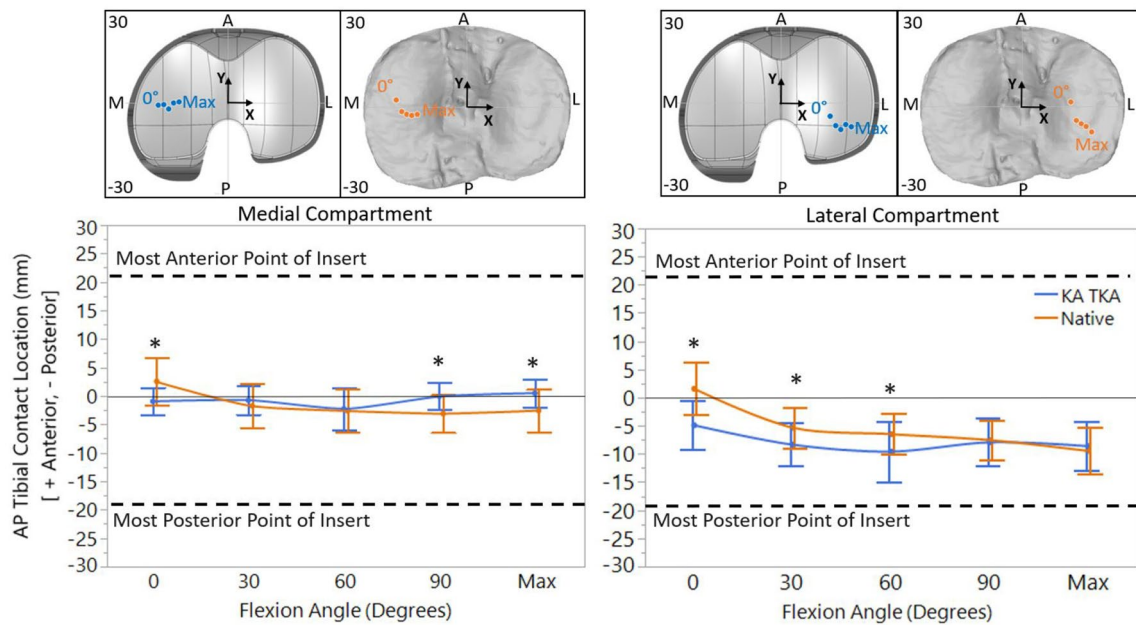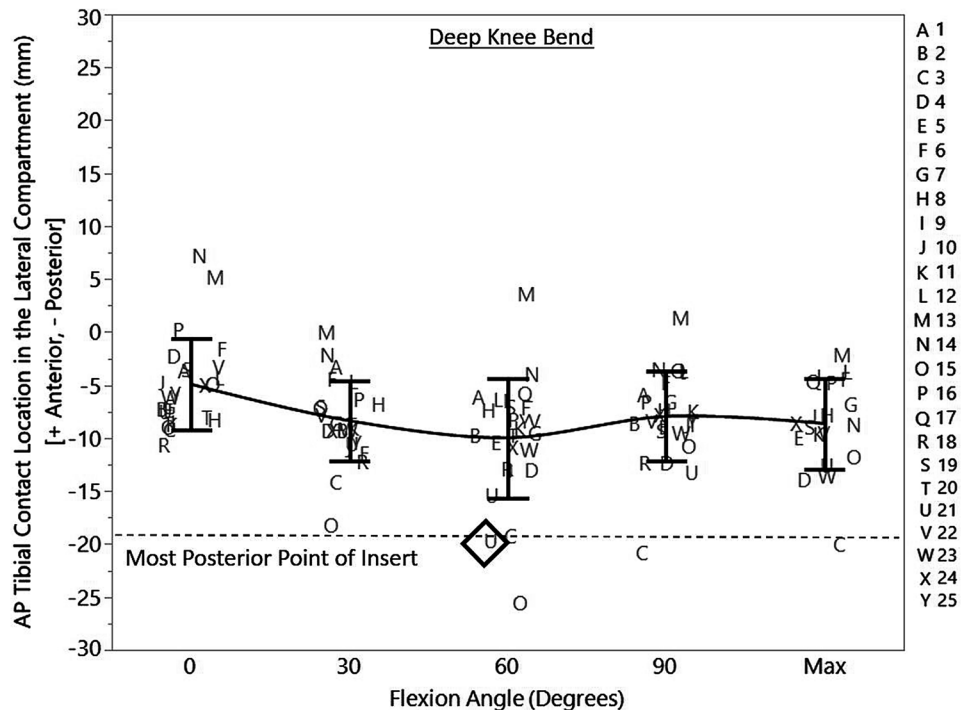
Fig. 3 Plots of the means and standard deviation of the AP tibial contact locations in the medial and lateral compartments of both KA TKA knees and native contralateral knees over flexion during a deep knee bend. The asterisks indicate statistically significant difference ($p < 0.05$). Insets (top) show the mean AP tibial contact locations in the medial and lateral compartments of the KA TKA knees and native contralateral knees at all flexion angles

Fig. 4 Anterior–posterior (AP) tibial contact locations in the lateral compartment of the KA TKA knees for each patient at each flexion angle during the deep knee bend. The dashed line indicates the most posterior point of the insert. The diamonds highlight posterior tibial contact locations that were corrected for bias error of 4.3 mm [29]. Posterior rim contact occurred for Patients C (3), O (15) and U (21)

flexion (Fig. 4). In contrast, posterior rim contact for Patient 15 developed earlier in flexion at 30° (Figs. 4, 5).

The incidence of posterior rim contact in the medial compartment was 4% (1 of 25 patients). As in the lateral compartment, posterior rim contact also developed in the medial compartment as Patient 15 reached 60° of flexion (Fig. 6).
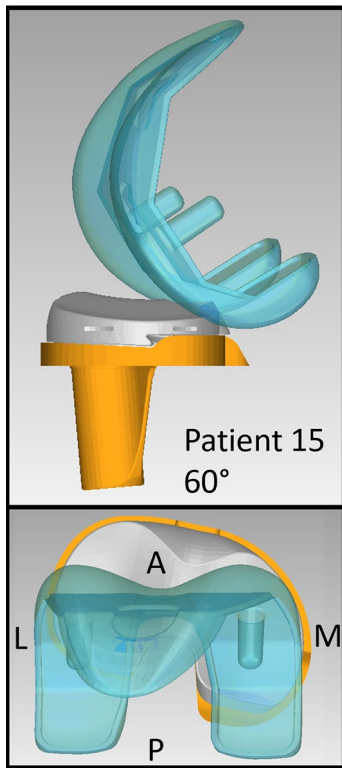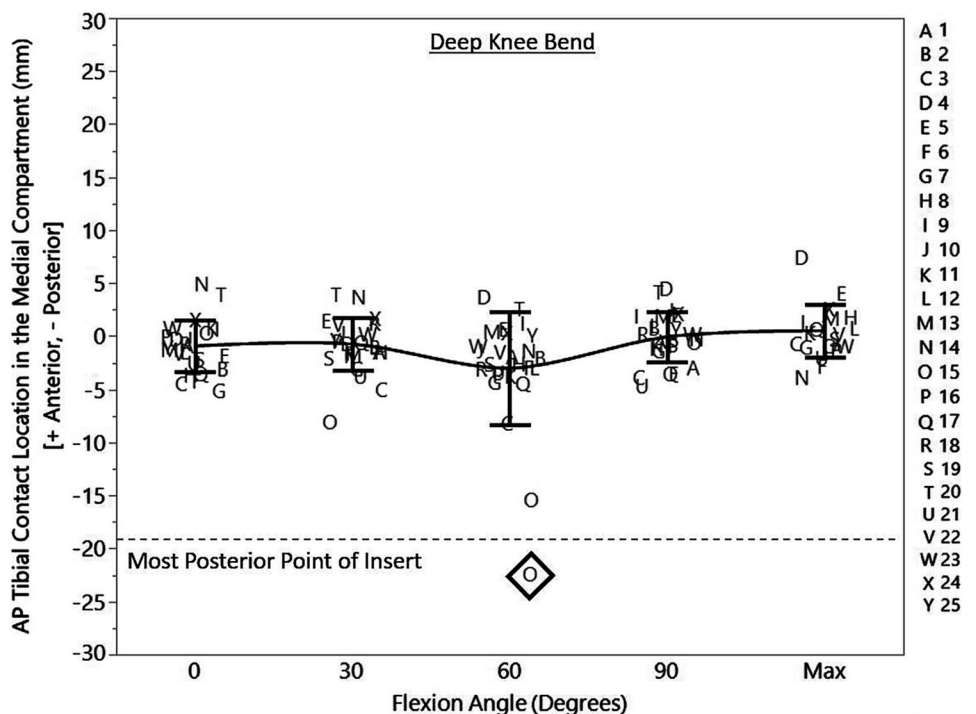
Fig. 5 Example of the position and orientation of the femoral and tibial components at a flexion angle where a patient exhibited posterior rim contact of the tibial insert during the deep knee bend in a lateral view (top) and axial superior view (bottom). The flexion angle shown is that where the tibial contact location was most posterior

Step-up

In the medial and lateral compartments at 0° of flexion, the mean AP tibial contact locations of the KA TKA knees were 6 mm and 8 mm more posterior than those of the native knees, respectively ($p < 0.0001$, $p < 0.0001$). At 15°, 30°, 45° and 60° of flexion, the differences in the mean AP tibial contact locations were 3 mm or less even when statistically significant (medial compartment 60°: $p = 0.0451$; lateral compartment 15°: $p = 0.0056$). Qualitatively, the mean AP tibial contact locations in the medial and lateral tibial compartments fell in the same regions between the KA TKA knees and the native knees at all flexion angles greater than 0° (Fig. 7).

The incidence of posterior rim contact of the tibial insert in the lateral compartment was 8% (2 of 25 patients). Posterior rim contact occurred initially at 60° flexion for Patient 3 and was maintained through 15° of flexion (Fig. 8). Posterior rim contact also was observed for Patient 20 which developed at 15° of flexion as the knee was extended. No patients exhibited posterior rim contact of the tibial insert in the medial compartment during a step-up.

ICC analysis

The ICC values for repeatability (i.e. intraobserver) and reproducibility (i.e. interobserver) for the native knee ranged from 0.76 to 0.85 for AP tibial contact locations in the medial compartment at 90° of flexion and in the lateral
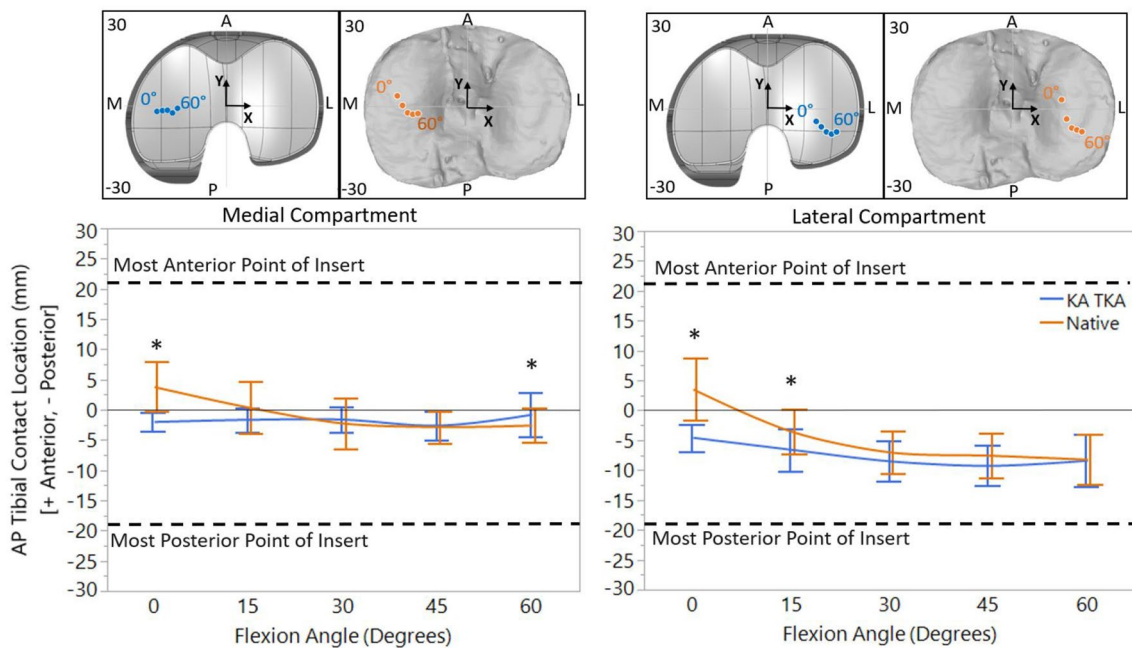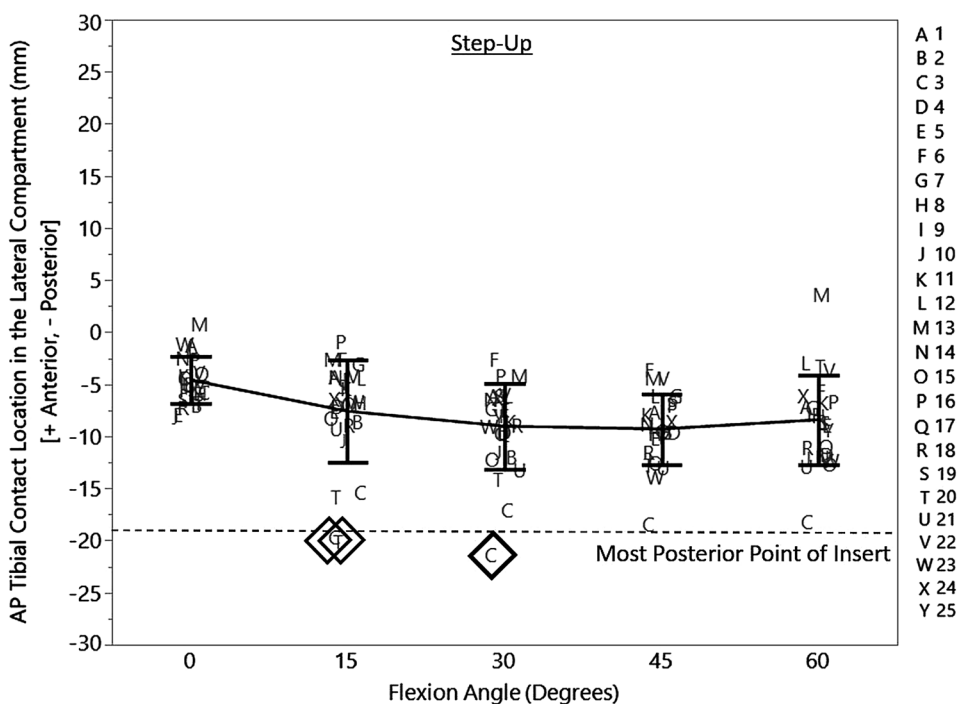
Fig. 6 Scatter plot shows the anterior–posterior (AP) tibial contact locations of the KA TKA knees in the medial compartment for each patient at each flexion angle during the deep knee bend. The dashed line indicates the most posterior point of the insert. The diamonds highlight posterior contact locations that were corrected for bias error of 7 mm [29]. Posterior rim contact occurred for Patient O (15)

Fig. 7 Plots of the means and standard deviation of the AP tibial contact locations in the medial and lateral compartments of both KA TKA knees and native contralateral knees over flexion during a step-up. The asterisks indicate statistically significant differences

($p < 0.05$). Insets (top) show the mean AP tibial contact locations in the medial and lateral compartments of the KA TKA knees and native contralateral knees at all flexion angles

Fig. 8 Anterior–posterior (AP) tibial contact locations in the lateral compartment of the KA TKA knees for each patient at each flexion angle during the step-up. The diamonds highlight posterior contact locations that were corrected for bias error of 4.3 mm. Posterior rim contact occurred for Patients C (3) and T (20)

compartment at 30° and 90° of flexion. The ICCs were 0.55 and 0.51 for repeatability and reproducibility, respectively, for AP tibial contact locations in the medial compartment at 30° of flexion. Accordingly, the repeatability

and reproducibility for the method for computing AP tibial contact locations in the native knee were rated as having moderate to good agreement. The repeatability errors for a representative observer were 1.7 mm and 1.1 mm for AP

tibial contact locations in the medial and lateral compartments in the native knees, respectively.

Discussion

The present study determined the differences in the AP tibial contact locations of a KA TKA knee performed with asymmetric, fixed bearing, PCR components from those of the native contralateral knee and also determined the incidence of posterior rim contact of the tibial insert during a deep knee bend and a step-up. The most important findings were that (1) the mean AP tibial contact locations were relatively centred in the compartments and differences between the KA TKAs and the native knees were limited to 2–8 mm, and (2) the incidence of posterior rim contact of the tibial insert was 16% (4 of 25 patients).

The differences in the mean AP tibial contact locations between the KA TKA knees and the native knees in the medial and lateral compartments were between 2 and 8 mm when statistically significant (Figs. 3, 7). However, these differences may not be clinically important in the context of their relationship to the 53 mm AP dimension of the mid-sized tibial plateau, which are approximately 15% or less. Further, the mean AP tibial contact locations of the KA TKA knees remained relatively centred in the AP direction in the medial and lateral compartments, similar to those of the native knees. Despite changes in stiffness and conformity of the articular surfaces and resection of the ACL which are inherent to TKA with PCR components, KA TKA produced mean AP tibial contact locations which were representative of those of the native contralateral knee during a deep knee bend and a step-up.

Although the mean AP tibial contact locations of the KA TKA knees were representative of those of the native contralateral knees, some differences merit discussion. The mean AP tibial contact locations of the KA TKA knees were somewhat posterior to those of the native contralateral knees in the medial and lateral compartments at full extension, and in the lateral compartment at 30° and 60° of flexion during a deep knee bend (Fig. 3). This was also observed during the step-up at full extension in both compartments and at 15° of flexion in the lateral compartment (Fig. 7). This behaviour may be partially explained by resection of the ACL which allows unopposed anterior pull of the patellar tendon on the tibia near extension. Further, resection of the ACL and replacement of the articular surfaces and menisci with implants of different stiffness and conformity may disrupt the screw-home mechanism resulting in less external rotation of the tibia on the femur in extension [19] which may partially explain the more posterior contact location in the lateral compartment compared to the medial compartment in the KA TKA knees (Figs. 3, 7).

The mean AP tibial contact locations of the KA TKA knees were anterior to those of the native contralateral knees in the medial compartment at 90° and maximum flexion during a deep knee bend (Fig. 3), and in the medial compartment at 60° of flexion during a step-up (Fig. 7). This may be partially explained by insufficient tension in the posterior cruciate ligament (PCL) allowing the femoral condyles to translate anteriorly on the tibia in deep flexion. These findings are consistent with the previous studies in MA TKA with PCR components which have shown anterior movement of the AP tibial contact locations with flexion [5, 8, 16, 33].

All four patients who developed posterior rim contact had high patient-reported outcome scores (e.g. Oxford Knee Scores ranging from 43 to 45), indicating that this behaviour did not adversely affect knee function at a follow-up of at least 2 years. However, this occurrence might cause accelerated wear. Intuitively, posterior rim contact would develop high Hertzian contact stresses when the AP contact location shifts from more centralised contact between conforming convex (femoral component) and concave (tibial insert) surfaces to line contact along the rim of the insert which offers no conformity with the articular surface of the femoral component. High Hertzian contact stresses in turn could lead to any one of a number of commonly observed failure mechanisms in inserts [9].

Not only were the outcome scores high for the patients who developed posterior rim loading, but also the outcome scores were high for the patient cohort as a whole (Table 2). Our outcome scores are comparable to those of other studies. For example, our mean Oxford Knee Score of 44 is equal to that from another study [24] and slightly greater than those of two other studies reporting means of 40 [6] and 42 [23]. Moreover, our high scores are expected to maintain in the long term since a 10-year follow-up reported a mean Oxford Knee Score of 43 [14].

Our findings confirm the efficacy of calipered KA TKA. Calipered KA TKA performed with asymmetric, fixed bearing, PCR components limited differences in mean AP tibial contact locations from native to approximately 15% of the AP depth of the mid-sized tibial baseplate. Qualitatively, the regions of the medial and lateral tibial compartments occupied by the mean AP tibial contact locations were similar to those of the native contralateral knee in mid- and late-flexion. These objective biomechanical results are consistent with the relatively high subjective patient-reported outcome scores herein and those previously reported for calipered KA TKA [6, 13, 23]. When viewed on the whole, our biomechanical results confirm the premise behind KA TKA that restoring the native limb and knee alignments without ligament release in turn limits the differences in AP tibial contact kinematics from native within the constraints of the particular component design used and leads to high patient-reported outcome scores.

Our findings also emphasise the need to look beyond basic statistics such as the mean and standard deviation in analysing results. If patient-specific results were not studied and only mean and standard deviation results were presented as in Figs. 3 and 7, then the occurrence of posterior rim contact in 16% (4 of 25) of patients would not have been evident. Accordingly, it is essential to view patient-specific results as presented in Figs. 5 and 8 so that the occurrence of biomechanical results characterising behaviour possibly leading to complications and the incidence of such results can be identified.

Two limitations merit discussion. First, this study considered one asymmetric, fixed bearing, PCR component design. It is well documented that component design and the presence or absence of the posterior cruciate ligament are important independent variables in the study of tibial contact kinematics [2, 25, 33, 34] so that these results may not be generalisable to KA TKA knees performed with different components. Second, the models used to compute AP tibial contact locations in the native contralateral knee were constructed from MRI images, which are known to underestimate bone morphology [28] and provide less contrast between bone and soft tissue, resulting in more noise and lower quality models than those constructed from high-resolution CT scans [21]. However, the method used for computing AP tibial contact locations in the native contralateral knee reduced the effects of noise and uncertainty in cartilage thickness by using the centroid of all points on the subchondral bone of the femoral condyles having a separation of 6 mm or less from the tibial subchondral bone [20].

A selection bias might have occurred if the patients who were imaged differed demographically from those who were not imaged. To assess this possibility, the pre-operative demographic data were compared statistically between the two groups of patients (Table 1). There were no statistically significant differences in the mean values of any parameter other than knee extension which differed by a few degrees. Given the close agreement in mean values of all demographic parameters in conjunction with the general lack of statistical significance, it is unlikely that differences in demographics introduced a selection bias.

Conclusion

Our biomechanical results confirm the premise that restoring the native limb and knee alignments without ligament release, in turn, limits the differences in mean AP tibial contact kinematics from native within the constraints of the particular component design used and generally restores high function as indicated by the patient-reported outcome scores. Although posterior rim contact in the lateral compartment of the tibial insert occurred for 16% (4 of 25) of patients, all 4 patients had high patient-reported outcome scores.

Compliance with ethical standards

Conflict of interest S. M. Howell is a paid consultant for THINK Surgical and Medacta, Inc. M. L. Hull receives research support from Zimmer-Biomet and Medacta, Inc. Remaining authors declare that they have no conflict of interest.

Ethical approval This study was approved by the University of California Davis Institutional Review Board (IRB#954288).

References

1. Banks SA, Hodge WA (1996) Accurate measurement of three-dimensional knee replacement kinematics using single-plane fluoroscopy. IEEE Trans Biomed Eng 43(6):638–649
2. Banks SA, Hodge WA (2004) Design and activity dependence of kinematics in fixed and mobile-bearing knee arthroplasties. J Arthroplast 19(7):809–816
3. Bartlett JW, Frost C (2008) Reliability, repeatability and reproducibility: analysis of measurement errors in continuous variables. Ultrasound Obstet Gynecol 31(4):466–475
4. Calliess T, Bauer K, Stukenborg-Colsman C, Windhagen H, Budde S, Ettinger M (2017) PSI kinematic versus non-PSI mechanical alignment in total knee arthroplasty: a prospective, randomized study. Knee Surg Sports Traumatol Arthrosc 25(6):1743–1748
5. Dennis DA, Komistek RD, Colwell CE Jr, Ranawat CS, Scott RD, Thornhill TS, Lapp MA (1998) In vivo anteroposterior femorotibial translation of total knee arthroplasty: a multicenter analysis. Clin Orthop Relat Res 356:47–57
6. Dossett HG, Estrada NA, Swartz GJ, LeFevre GW, Kwasman BG (2014) A randomised controlled trial of kinematically and mechanically aligned total knee replacements: two-year clinical results. Bone Jt J 96-B(7):907–913
7. Fregly BJ, Rahman HA, Banks SA (2005) Theoretical accuracy of model-based shape matching for measuring natural knee kinematics with single-plane fluoroscopy. J Biomech Eng 127(4):692–699
8. Grieco TF, Sharma A, Komistek RD, Cates HE (2016) Single versus multiple-radii cruciate-retaining total knee arthroplasty: an in vivo mobile fluoroscopy study. J Arthroplast 31(3):694–701
9. Harman MK, Banks SA, Hodge WA (2001) Polyethylene damage and knee kinematics after total knee arthroplasty. Clin Orthop Relat Res 393:383–393
10. Hess S, Moser LB, Amsler F, Behrend H, Hirschmann MT (2019) Highly variable coronal tibial and femoral alignment

in osteoarthritic knees: a systematic review. Knee Surg Sports Traumatol Arthrosc. https://doi.org/10.1007/s00167-00019-05506-00162

11. Hirschmann MT, Moser LB, Amsler F, Behrend H, Leclerq V, Hess S (2019) Functional knee phenotypes: a novel classification for phenotyping the coronal lower limb alignment based on the native alignment in young non-osteoarthritic patients. Knee Surg Sports Traumatol Arthrosc. https://doi.org/10.1007/s00167-00019-05509-z

12. Howell SM, Hodapp EE, Vernace JV, Hull ML, Meade TD (2013) Are undesirable contact kinematics minimized after kinematically aligned total knee arthroplasty? An intersurgeon analysis of consecutive patients. Knee Surg Sports Traumatol Arthrosc 21(10):2281–2287

13. Howell SM, Papadopoulos S, Kuznik KT, Hull ML (2013) Accurate alignment and high function after kinematically aligned TKA performed with generic instruments. Knee Surg Sports Traumatol Arthrosc 21(10):2271–2280

14. Howell SM, Shelton TJ, Hull ML (2018) Implant survival and function ten years after kinematically aligned total knee arthroplasty. J Arthroplast. https://doi.org/10.1016/j.arth.2018.07.020

15. Indrayan A (2013) Methods of clinical epidemiology. Springer series on epidemiology and public health, Chap 2. Springer, Berlin. https://doi.org/10.1007/978-3-642-37131-8_2

16. Li C, Hosseini A, Tsai TY, Kwon YM, Li G (2015) Articular contact kinematics of the knee before and after a cruciate retaining total knee arthroplasty. J Orthop Res 33(3):349–358

17. Mahfouz MR, Hoff WA, Komistek RD, Dennis DA (2003) A robust method for registration of three-dimensional knee implant models to two-dimensional fluoroscopy images. IEEE Trans Med Imaging 22(12):1561–1574

18. Matsumoto T, Takayama K, Ishida K, Hayashi S, Hashimoto S, Kuroda R (2017) Radiological and clinical comparison of kinematically versus mechanically aligned total knee arthroplasty. Bone Jt J 99-B(5):640–646

19. Moglo KE, Shirazi-Adl A (2005) Cruciate coupling and screw-home mechanism in passive knee joint during extension–flexion. J Biomech 38(5):1075–1083

20. Moro-oka TA, Hamai S, Miura H, Shimoto T, Higaki H, Fregly BJ, Iwamoto Y, Banks SA (2008) Dynamic activity dependence of in vivo normal knee kinematics. J Orthop Res 26(4):428–434

21. Moro-oka T, Hamai S, Miura H, Shimoto T, Higaki H, Fregly BJ, Iwamoto Y, Banks SA (2007) Can magnetic resonance imaging–derived bone models be used for accurate motion measurement with single-plane three-dimensional shape registration? J Orthop Res 25(7):867–872

22. Moser LB, Hess S, Amsler F, Behrend H, Hirschmann MT (2019) Native non-osteoarthritic knees have a highly variable coronal alignment: a systematic review. Knee Surg Sports Traumatol Arthrosc. https://doi.org/10.1007/s00167-00019-05417-00162

23. Nedopil AJ, Howell SM, Hull ML (2016) Does malrotation of the tibial and femoral components compromise function in kinematically aligned total knee arthroplasty? Orthop Clin N Am 47(1):41–50

24. Nedopil AJ, Singh AK, Howell SM, Hull ML (2018) Does calipered kinematically aligned TKA restore native left to right symmetry of the lower limb and improve function? J Arthroplast 33(2):398–406

25. Okamoto N, Breslauer L, Hedley AK, Mizuta H, Banks SA (2011) In vivo knee kinematics in patients with bilateral total knee arthroplasty of 2 designs. J Arthroplast 26(6):914–918

26. Paschos NK, Howell SM, Johnson JM, Mahfouz MR (2017) Can kinematic tibial templates assist the surgeon locating the flexion and extension plane of the knee? Knee 24(5):1006–1015

27. Prins AH, Kaptein BL, Stoel BC, Reiber JHC, Valstar ER (2010) Detecting femur–insert collisions to improve precision of fluoroscopic knee arthroplasty analysis. J Biomech 43(4):694–700

28. Rathnayaka K, Momot KI, Noser H, Volp A, Schuetz MA, Sahama T, Schmutz B (2012) Quantification of the accuracy of MRI generated 3D models of long bones compared to CT generated 3D models. Med Eng Phys 34(3):357–363

29. Ross DS, Howell SM, Hull ML (2017) Errors in calculating anterior–posterior tibial contact locations in total knee arthroplasty using three-dimensional model to two-dimensional image registration in radiographs: an in vitro study of two methods. J Biomech Eng 139(12):121003.121001–121003.121010

30. Roth JD, Howell SM, Hull ML (2015) Native knee laxities at 0, 45, and 90 of flexion and their relationship to the goal of the gap-balancing alignment method of total knee arthroplasty. J Bone Jt Surg 97-A(20):1678–1684

31. Roth JD, Howell SM, Hull ML (2018) Kinematically aligned total knee arthroplasty limits high tibial forces, differences in tibial forces between compartments, and abnormal tibial contact kinematics during passive flexion. Knee Surg Sports Traumatol Arthrosc 26(6):1589–1601

32. Roth JD, Howell SM, Hull ML (2019) Analysis of differences in laxities and neutral positions from native after kinematically aligned TKA using cruciate retaining implants. J Orthop Res 37(2):358–369

33. Victor J, Banks S, Bellemans J (2005) Kinematics of posterior cruciate ligament-retaining and -substituting total knee arthroplasty: a prospective randomized outcome study. J Bone Jt Surg 87-B(5):646–655

34. Watanabe T, Ishizuki M, Muneta T, Banks SA (2013) Knee kinematics in anterior cruciate ligament-substituting arthroplasty with or without the posterior cruciate ligament. J Arthroplast 28(4):548–552

35. Yamaguchi S, Gamada K, Sasho T, Kato H, Sonoda M, Banks SA (2009) In vivo kinematics of anterior cruciate ligament deficient knees during pivot and squat activities. Clin Biomech 24(1):71–76